Supporting Information

Nagai et al. 10.1073/pnas.1110013108

SI Materials and Methods

Characterization of Fibers. The lengths and widths of each fiber were determined by measuring at least 1,000 fibers with a high-resolution optical microscope (BZ-8000; Keyence) and a transmission electron microscope (JEM1400EX; JEOL). For the optical images, suspended fibers were spread over a glass slide, and a high-N.A. (1.40) lens was used. For transmission EM images, saline solution containing 0.5% BSA (A-saline solution)-suspended multiwalled carbon nanotubes (MWCNTs) and saline solution-suspended asbestos were spread directly over a copper grid with a plastic mesh and a carbon coat (cat. no. 653; Nisshin EM). After drying, fibers were analyzed. High-resolution transmission EM images were taken on a JEM-2100F (JEOL) high-resolution field-emission gun transmission electron microscope operated at 80 keV at room temperature under a pressure of 10^{-6} Pa. To determine the number of dispersed fibers in suspension, 0.5 mg/mL of the fiber suspensions was diluted to 0.05 mg/mL in saline containing 0.5% albumin. The diluted solution was then observed under a light microscope (BZ-8000). We counted the number of fibers inside a square with sides of 250 μm. In total, at least 16 fields of view were analyzed for each fiber type, and the concentration was calculated.

Establishment of a Mesothelial Cell Line. Human peritoneal mesothelial cells (HPMCs) were cultured from a resected omentum without peritoneal dissemination of an ovarian cancer patient as previously described (1). Written permission was obtained, and the procedure was approved by the Committee for Bioethics of the Nagoya University Graduate School of Medicine. The cells were grown in RPMI medium 1640 containing 10% FBS. The retroviral vectors, pCMSCVpuro-16E6E7 and pCMSCVneo-hTERT, were constructed by recombining segments of donor vectors (gifts from Tohru Kiyono, National Cancer Center, Tokyo, Japan) containing full-length HPV16E6 and E7 and the catalytic unit of human telomerase (2) using the Gateway system (Invitrogen) as previously described (3). Retroviral vectors encoding mCherry-human β-actin were produced by amplifying plasmid DNA from pmCherry-actin using PCR and the same set of primers. For attB1EGFPCherryCF, we used 5′-AAAAAGCAGGCTCCACCATGGTGAGCAAGGGCGA-3′ and attB2actinR 5′- AGAAAGCTGGGCTAGAAGCATTTGCGGTGGA-3′ and the adaptor primers 5′-GGGGACAAGTTTGTACAAAAAAGCAGGCT-3′ and 5′-GGGGACCACTTTGTACAAGAAAGCTGGGT-3′. After confirming the sequence, the Gateway system was used to generate pCMSCVneo mCherry-actin. HPMCs were infected at day 21 of culture with recombinant retroviruses containing E6 and E7 or mCherry-actin with the 10A1 envelope using 4 μg/mL Polybrene. Drug selection was then performed with 1 μg/mL puromycin or 0.2 mg/mL G418. For combinations of retroviral infections, E6 and E7-transduced cells were subsequently infected with the pCMSCVneo-hTERT-10A1 virus and then selected with G418.

Transmission EM to Evaluate Fiber Localization. We grew cells at 1×10^4 cells/cm^2 at 1 d before the addition of each fiber. Fibers were added at 5 μg/cm^2. The cells were fixed in phosphate buffer containing 2.5% glutaraldehyde and 2% paraformaldehyde after a 3-h incubation. The cells were then fixed with 1% osmium tetroxide and embedded in Epon resin, which was cut by a diamond knife into 80-nm or 500-nm ultrathin sections. The specimens were observed with a transmission electron microscope (JEM-1400EX; JEOL). Localization of fibers was determined by counting at least 30 randomly selected cells three times. In total, at least 100 cells were observed in each group.

Scanning EM to Evaluate Fiber Localization. We grew cells at 1×10^4 cells/cm^2 at 1 d before the addition of each fiber. Fibers were added at 5 μg/cm^2 and fixed in phosphate buffer containing 2% glutaraldehyde after a 3-h incubation. Cells were then rinsed, treated with 1% tannic acid and fixed again with 2% osmium tetroxide. Finally, cells were coated with osmium tetroxide at a thickness of 10 nm and observed with a scanning electron microscope (S-800S; Hitachi).

Cell Viability Assay Using Serum-Treated Fibers. Preparation of serum-treated fibers was performed by mixing equal amounts of FBS with the fiber suspension (0.5 mg/mL) at 37 °C for 30 min. The mixture was then centrifuged at 15,000 × *g* at 4 °C for 10 min, and the supernatants were discarded. The pellets were then suspended in culture medium.

Determination of Metal Concentrations. To measure the metals in the fiber suspensions, the supernatants were collected using the following procedure: centrifugation of the A-saline solution–suspended MWCNTs or saline-suspended asbestos (0.5 mg/mL) at 15,000 × *g* at 4 °C for 10 min, followed by careful collection of the supernatant and another centrifugation and collection step. For NT50a, NT50b, NT115, NT145, chrysotile (Chry), crocidolite (Cro), and amosite (Amo), we repeated the centrifugation and again collected the supernatant. For NTtngl, we performed ultracentrifugation at 300,000 × *g* at 4 °C for 30 min and collected the supernatant. The final supernatants were diluted 1:5 with deionized water. To measure the metals in the samples, 1 mL of each sample solution was completely reduced to ash by repeated treatment with nitric acid, hydrogen peroxide, and perchloric acid under heating at 200 °C. The sample ashes were dissolved in 9 mL of 7% nitric acid and then analyzed by inductively coupled plasma-MS by using an ICPM-8500 mass spectrometer (Shimadzu). We first measured magnesium, zinc, chromium, lead, nickel, and cadmium qualitatively and confirmed that the concentration of these metals in each sample was less than 10 ng/mL. Next, we measured the iron content (*m*/*z* 57) and the levels of copper (*m*/*z* 65). The concentration of both metals in each sample was calculated by using a standard curve for Fe and Cu (Wako). Values of a serially diluted standard solution displayed a linear regression with a straight line ranging from 10 to 100 ng/mL (ppb) for iron and from 1 to 100 ng/mL for copper. The measurement was performed at least five times (n = 5) to verify the results.

Electron Paramagnetic Resonance. We used an electron paramagnetic resonance spectrometer (JES-FR30; JEOL) to evaluate the free radical generation from each fibrous particle in the presence of hydrogen peroxide according to a previously described method (4) with slight modifications. The instrument settings were as follows: microwave frequency, 9.425 GHz; microwave power, 4 mW; modulation frequency, 100 kHz; modulation amplitude, 0.079 mT; sweep width, 5 mT; sweep time, 30 s; time constant, 0.1 s; center magnetic field, 336.2 mT and temperature, 290 K. We recorded the spectrum of the spin-trapped signals produced after 30 min of incubation at 37 °C. The reaction mixture was prepared by consecutively adding 20 μL of PBS solution (100 mM, pH 7.4), 60 μL of nitrilotriacetic acid disodium salt (5 mM), 80 μL of fiber suspension (5 mg/mL), 20 μL of 5,5-dimethyl-1-pyrroline-*N*-oxide (90 mM), and 20 μL

of hydrogen peroxide (100 mM). RDC-60-S disposable syringes (Radical Research) were used for the measurements.

Protein Adsorption on Fibers. We performed immunoprecipitation-like assay as previously described (5). FBS (100 μL) and each fiber (250 μg) were mixed, and RIPA (20 mM Tris-HCl, pH 7.4, 0.1% SDS, 1% Triton X-100, and 1% sodium deoxycholate) was added up to 1 mL In the case of HPMC lysate, 50 μg of cell lysate was mixed with each fiber suspension instead of serum. After a 3-h incubation at 37 °C, the mixture was centrifuged (15,000 X *g*) at 4 °C for 5 min. The supernatants were discarded, and the pellets were resuspended in RIPA buffer followed by two more cycles of centrifugation and resuspension. After the final centrifugation, we carefully discarded all supernatants, added SDS sample buffer, and boiled the samples for 10 min. The samples were centrifuged (15,000 × *g*) at 4 °C for 2 min, and the supernatants were evaluated by SDS/PAGE. The gel was silver-stained using a kit (Silver Staining Kit, Protein; GE Healthcare).

Fluorescent Images of Cellular Uptake of Fibers. MeT5A cells were cotransfected with actin-EGFP and either wild-type (WT) (6) or an inactive form (S34N) (7) of rab5a by using Lipofectamine 2000 (Invitrogen). The SSC value of EGFP-positive cells was then measured. The HPMCs were transfected with rab5a-GFP (Organelle Lights; Invitrogen) and actin-mCherry and observed under a fluorescent microscope (BZ-8000) at 5-min intervals after the addition of Cro, NT50a, and NT145. Representative images are shown in Fig. S1.

Raman Spectrometry. Raman spectra were measured in the backscattering geometry by using a single monochromator and a microscope (HR-800; Horiba/Jobin Yvon) equipped with a CCD detector and a notch filter. The sample was excited by a He-Ne laser at 633 nm.

Quantitative RT-PCR Analysis. We grew RAW264.7 macrophages at a density of 5×10^4 cells/cm^2 at 1 d before the addition of each fiber. For each experiment, fibers were added to the culture medium to a final concentration of 0.1, 1 or 5 μg/cm^2. After 24 h, the total RNA was extracted with an RNeasy Plus Mini kit (Qiagen), and the cDNA was synthesized using the random primers, reverse transcriptase and buffer included in an RNA PCR kit (AMV; version 3.0; Takara). We used Platinum SYBR Green qPCR SuperMix-UDG (Invitrogen) and a 7300 real-time PCR system (Applied Biosystems) to conduct quantitative PCR. The expression of each mRNA (TNF-α, IL-1β, and IL-6) was normalized using 18S rRNA. The results show relative mRNA abundance compared with the control group. The primers used are as follows: 18S rRNA, sense (TCCTTTGGTCGCTCGCTCCT) and antisense (TGCTGCCTTCCTTGGATGTG); TNF-α, sense (GTGCCTATGTCTCAGCCTCT) and antisense (CTCCTCCACTTGGTGGTTTG); IL-1β, sense (CTCAACTGTGAAATGCCACC) and antisense (GAGTGATACTGCCTGCCTGA); IL-6, sense (CTTCTTGGGACTGATGCTGG) and antisense (CAGAATTGCCATTGCACAAC).

Immunohistochemical Analysis of Mesotheliomas. We prepared tissue arrays and performed immunohistochemistry as previously described (8, 9). Briefly, cores of 3 mm in diameter at representative areas were punched out, and six or 24 cores were embedded in a paraffin block that was sliced into 4-μm sections. We dewaxed sections that were attached onto slides in xylene and ethanol and subjected them to high-temperature antigen retrieval in an Immunosaver (Nisshin EM) for 40 min. After antigen retrieval, the slides were dipped in methanol containing H_2O_2 (0.3% vol/vol) to quench endogenous peroxidase activity for 30 min. After washing with PBS solution, slides were incubated with primary antibodies and washed with PBS solution three times for 5 min each. SimpleStain Rat multi (Nichirei) was applied to the slides followed by three washes with PBS solution. Localization of antigen-antibody complexes was visualized by liquid DAB+ (Dako) as brown precipitates before nuclear counterstaining with hematoxylin. Primary antibodies were as follows: anti–S-100 polyclonal antibody (LSL-LB-9197) was from Cosmo Bio, antidesmin monoclonal antibody (clone D33) was from Dako, antipodoplanin polyclonal antibody (KS-17) was from Sigma, anti-pan-cytokeratin monoclonal antibody (clone AE1/AE3) was from Thermo Fisher Scientific, and anti-mesothelin polyclonal antibody was from IBL (Immuno Biological Laboratories). Only in the case of desmin staining did we skip the antigen retrieval step.

Time-Lapse Microscopy. We grew MeT5A mesothelial cells or RAW 264.7 macrophages at 1×10^4 cells/cm^2 at 1 d before the addition of each fiber. Fibers were added at 5 μg/cm^2, and images were taken every minute for 3 to 4 h. The movies were made at a frame rate of 8 frames per second.

1. Kajiyama H, et al. (2008) Involvement of SDF-1alpha/CXCR4 axis in the enhanced peritoneal metastasis of epithelial ovarian carcinoma. *Int J Cancer* 122:91–99.
2. Okamoto T, et al. (2002) Clonal heterogeneity in differentiation potential of immortalized human mesenchymal stem cells. *Biochem Biophys Res Commun* 295: 354–361.
3. Yamashita Y, Tsurumi T, Mori N, Kiyono T (2006) Immortalization of Epstein-Barr virus-negative human B lymphocytes with minimal chromosomal instability. *Pathol Int* 56: 659–667.
4. Jiang L, et al. (2008) Characteristics and modifying factors of asbestos-induced oxidative DNA damage. *Cancer Sci* 99:2142–2151.
5. Nagai H, et al. (2011) Asbestos surface provides a niche for oxidative modification. *Cancer Sci*, 10.1111/j.1349-7006.2011.02087.
6. Tsuboi T, Fukuda M (2006) Rab3A and Rab27A cooperatively regulate the docking step of dense-core vesicle exocytosis in PC12 cells. *J Cell Sci* 119:2196–2203.
7. Tamura K, et al. (2009) Varp is a novel Rab32/38-binding protein that regulates Tyrp1 trafficking in melanocytes. *Mol Biol Cell* 20:2900–2908.
8. Hu Q, et al. (2010) Homozygous deletion of CDKN2A/2B is a hallmark of iron-induced high-grade rat mesothelioma. *Lab Invest* 90:360–373.
9. Okazaki Y, et al. (2010) A beverage containing fermented black soybean ameliorates ferric nitrilotriacetate-induced renal oxidative damage in rats. *J Clin Biochem Nutr* 47:198–207.

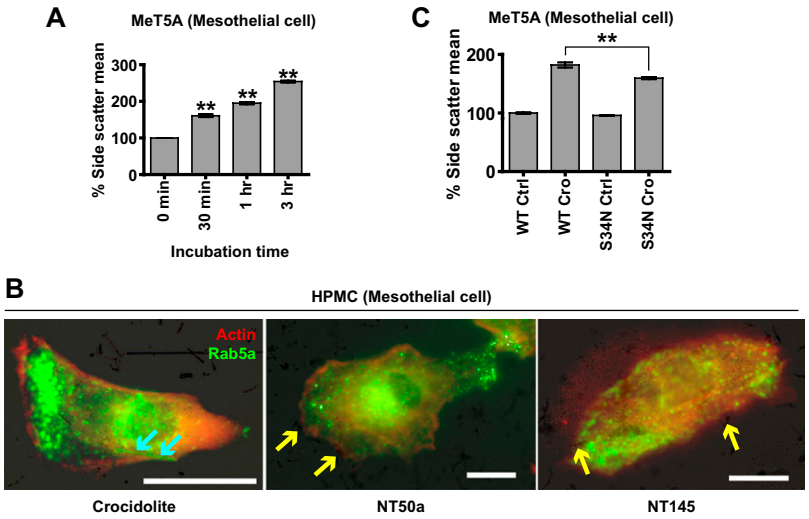

Fig. S1. Cro was internalized by mesothelial cells by an active signaling pathway that included rab5a. (*A*) Time-dependent increase in side scatter value of MeT5A cells after incubation with Cro. *P* values were calculated between 0 min (no addition of Cro) and the indicated times. (*B*) HPMCs transfected with rab5a-GFP and actin-mCherry internalized Cro with rab5a recruitment but did not internalize NT50a or NT145. Blue arrows indicate rab5a recruitment around the asbestos fiber whereas yellow arrows indicate lack of rab5a around nanotubes. (Scale bars: 20 μm.) (*C*) Mean of the side scatter value of each cell after a 3-h incubation with control (saline) or Cro. A partial inhibition of the increase in SSC value via cotransfection of the inactive form of rab5a (S34N) and actin-EGFP into MeT5A cells (**$P < 0.01$; $n = 3$, mean ± SEM). *P* values were determined by one-way ANOVA with post-hoc Tukey test.

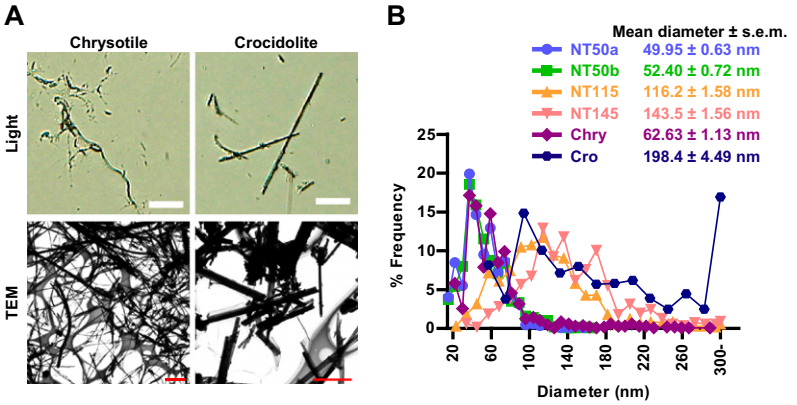

Fig. S2. Supplementary data for fiber diameter. (*A*) Optical images and transmission EM (TEM) images of Chry and Cro. (Scale bars: light microscopy images, 20 μm; transmission EM images, 2 μm.) (*B*) Distribution of the diameters of MWCNTs and asbestos.

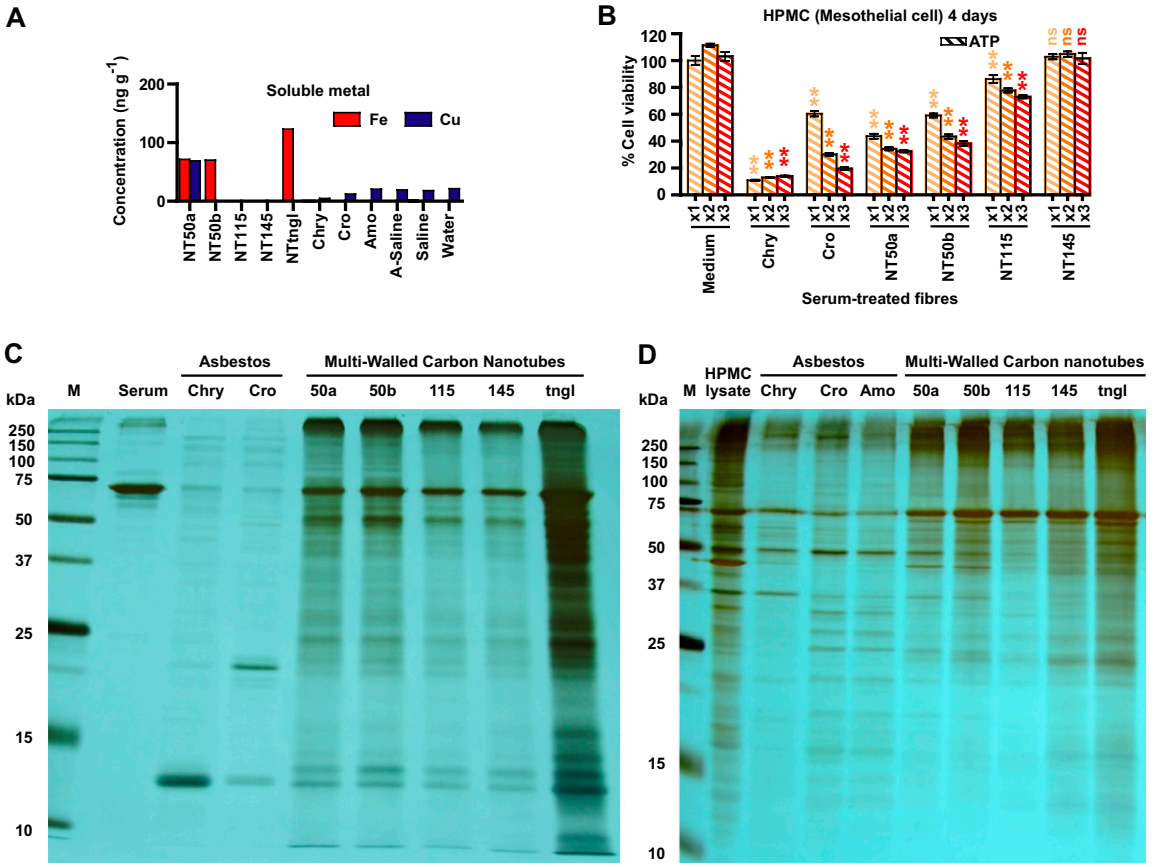

Fig. S3. Neither contaminating metals, serum depletion by fiber surface, nor protein adsorptive activity were the primary causes of mesothelial cell cytotoxicity by thin, dispersed MWCNTs with high crystallinity and rigidity. (*A*) Soluble metal (Fe and Cu) in each fiber solution (0.5 mg/mL). (*B*) ATP viability assay for HPMCs incubated with serum-treated fibers shows that NT50a (diameter ~ 50 nm) was severely cytotoxic, but NT145 (diameter ~ 150 nm) lacked cytotoxicity even at a density of 15 μg/cm^2 ($n = 4$, mean ± SEM; $^{**}P < 0.01$; ns, not significant). *P* values were determined by one-way ANOVA with post-hoc Tukey test. (*C* and *D*) Silver-stained gel after SDS/PAGE. Protein bands represent adsorptive proteins on the surface of the fibers (M, marker). Serum (*C*) and HPMC lysate (*D*) represent the original pattern. Each MWCNT type showed a similar profile in protein adsorption, but there was a difference in the amount of the adsorbed proteins. FBS (*C*) and HPMC lysate (*D*) were incubated with fibers as described in *SI Materials and Methods*.

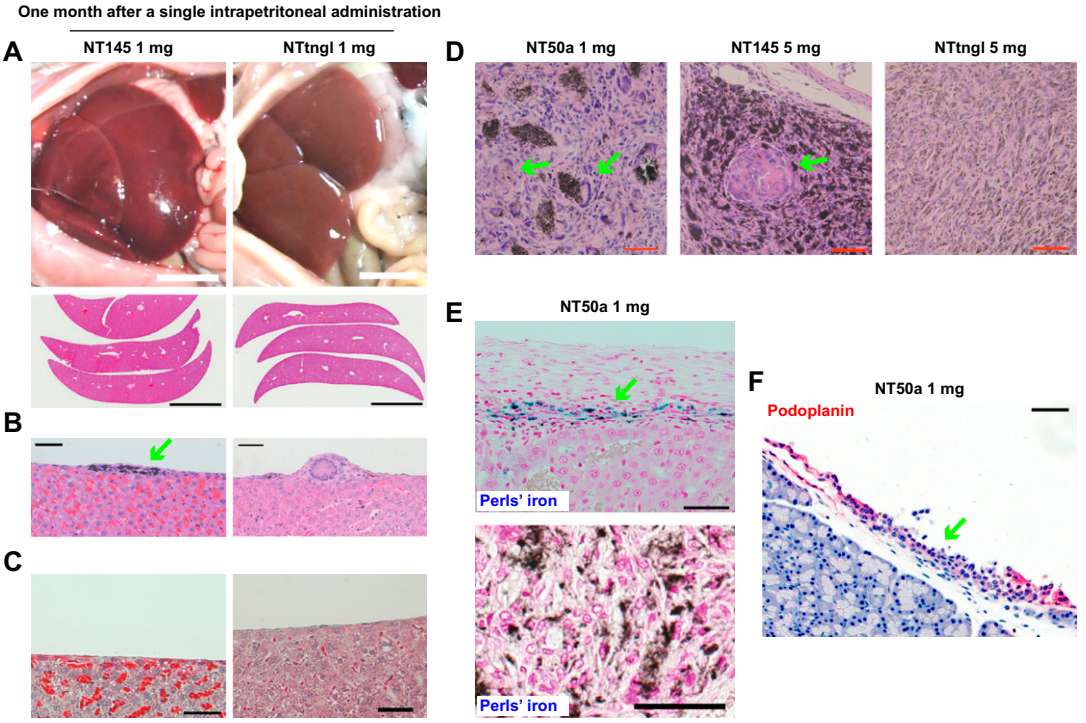

Fig. S4. NT50a uniquely induced iron deposition inside fibrotic tissue and mesothelial proliferation. (*A*–*C*) Macroscopic and microscopic images of rat organs 1 mo after a single i.p. injection of 1 mg NT145 (*Left*) or 1 mg NTtngl (*Right*). (*A*) Macroscopic images of i.p. organs just after dissection (*Top*). Low-power view of H&E-stained livers (*Bottom*). (Scale bars: 1 cm.) (*B*) Microscopic images of liver surface show the deposition of fibers (arrow) and little fibrotic responses around fibers. (*C*) Masson trichrome staining showing scarce light-green collagen. (*D*) Granuloma with multinuclear giant cells (arrow). (*E*) Perls' iron staining (blue) shows iron deposition (*Upper*, arrow) and shows that NT50a nanotubes are not stained (*Lower*) and thus that iron deposition (*Upper*) is a result of internal iron. (*F*) Immunohistochemistry for podoplanin (red) shows proliferation of mesothelial cells (arrow) in NT50a-injected rats. (Scale bars: *B*–*E*, 50 μm; *F*, 100 μm.)

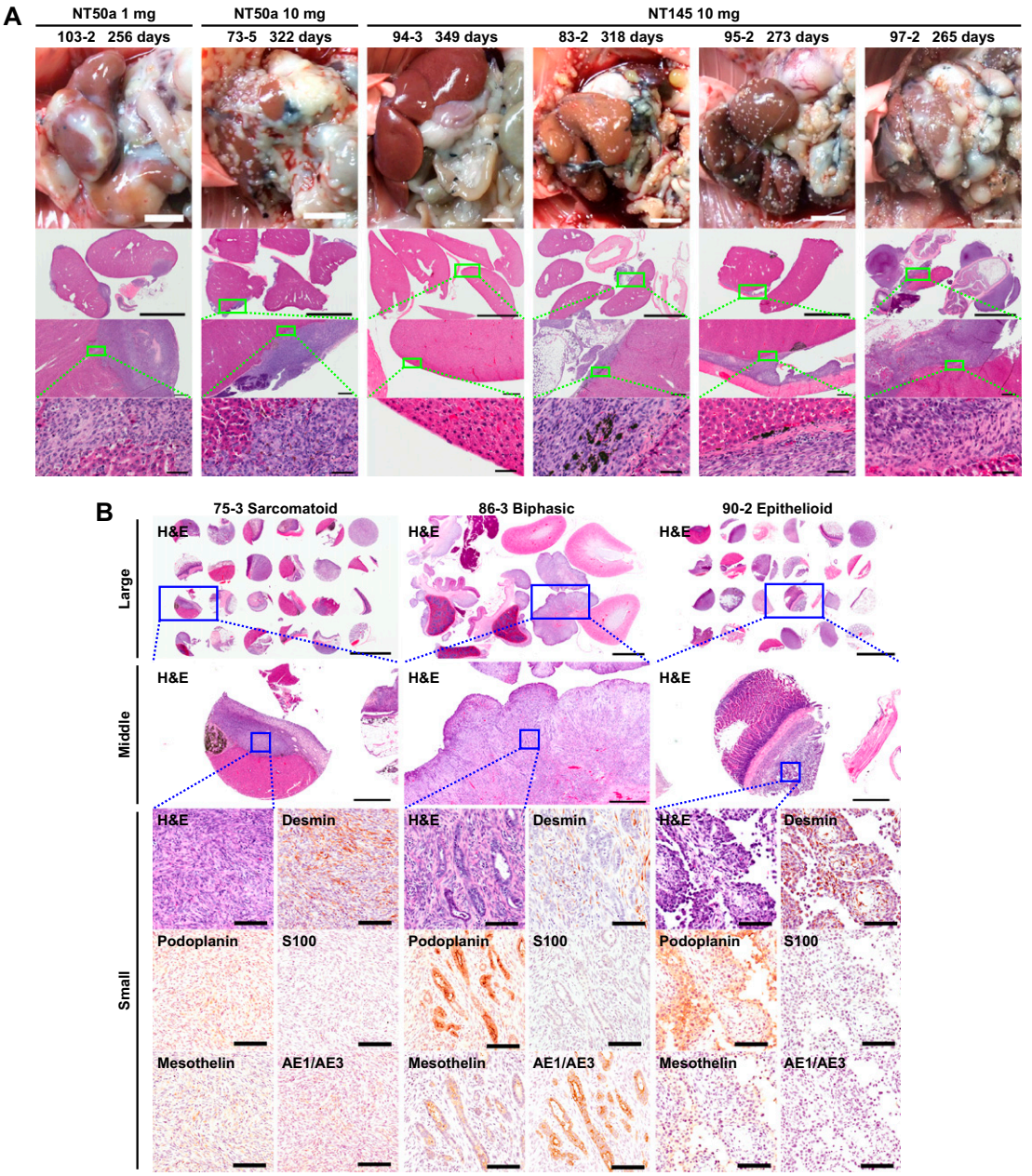

Fig. S5. Histopathology of mesothelioma. (*A*) Macroscopic images of i.p. organs just after dissection (*Top*). Low-power view of H&E-stained livers and other organs (*Bottom*). Microscopic images of mesothelioma invading liver parenchyma (103-2 and 73-5). Mesothelioma was not found in 94-3. Various extent of mesothelioma growth in rats injected with 10 mg NT145 (83-2, 95-2, and 97-2). (Scale bars: from top to bottom, 1 cm, 1 cm, 500 μm, and 50 μm.) (*B*) Immunohistochemistry of each specimen. (Scale bars: large, 5 mm; medium, 1 mm; small, 100 μm.)

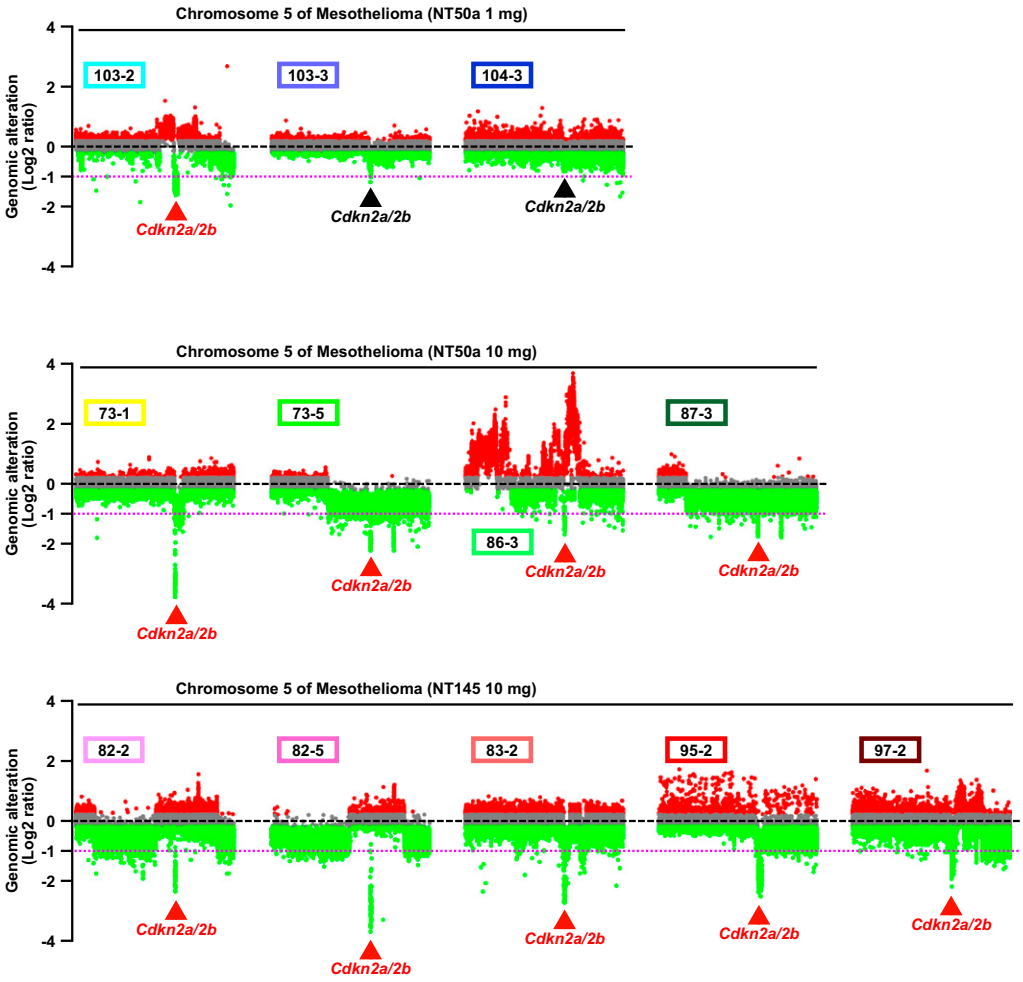

Fig. S6. *Cdkn2a/2b* was deleted in mesotheliomas induced by MWCNTs. Full scatter plot data for rat chromosome 5 indicates homozygous or heterozygous deletion of *Cdkn2a/2b*. Pink dotted lines decide whether the genomic deletion is homozygous ($y < -1$) or heterozygous. Red triangles indicate homozygous and black triangles indicate heterozygous or homozygous deletion. The numbers in squares indicate the identification number.

Table S1. Overall summary table of characteristics of MWCNTs

Characteristic*	NT50a	NT50b	NT115	NT145	NTtngl
Manufacturer	Mitsui	Showa Denko	Showa Denko	Showa Denko	Showa Denko
Diameter by the company, nm	50	80	150	150	15
Diameter by authors, nm	49.95 ± 0.63	52.4 ± 0.72	116.2 ± 1.6	143.5 ± 1.6	ND
Length by the company, μm	4	10	8	6	3
Length by authors, μm	5.29 ± 0.12	4.6 ± 0.10	4.88 ± 0.10	4.34 ± 0.08	ND
Aggregation extent	High	High	Low	Low	Very high
G/D ratio	6.7 ± 0.34	9.5 ± 1.0	7.0 ± 0.6	5.5 ± 0.6	1.5 ± 0.1
ROS generation via EPR (S/M)	0.27 ± 0.01	0.14 ± 0.03	0.20 ± 0.07	0.13 ± 0.03	0.24 ± 0.01
Phagocytosis by macrophages	Yes	Yes	Yes	Yes	None
Toxicity to macrophages	Moderate	Moderate	Moderate	Moderate	Very low
Piercing mesothelial cell membrane	Yes	ND	Low	Very low	None
Toxicity to mesothelial cells	High	High	Low	Low	Low
Inflammogenicity to rats	High	ND	ND	Low	Low
Carcinogenicity to rats	High	High	ND	Low	None

Values presented as mean ± SEM where applicable. EPR, electron paramagnetic resonance; G/D, graphite/defect; ND, not determined; ROS, reactive oxygen species; S/M, signal to marker ratio.
*0.5 mg/mL in A-saline solution.

Table S2. Mesotheliomagenesis experiment

	Female		Male		Total		Histology		
Name/dose, mg	Alive	Dead	Alive	Dead	Alive	Mesothelioma	Epithelioid	Biphasic	Sarcomatoid
NT50a									
-agg*	15	0	ND	ND	15	12	0	2	10
1	9	0	4	0	13	13	0	0	13
10[†]	23	12	20	5	43	43	1	7	34
NT50b									
10	6	5	ND	ND	6	6	0	1	5
NT145									
1	14	0	15	0	29	5	0	0	5
10	18	15	12	6	30	28	0	3	25
NTtngl									
10	9	4	6	6	15	0	0	0	0
A-saline (control)									
0	15	0	8	0	23	0	0	0	0

ND, not done; A-saline is vehicle control.
[†]Histological analysis was not possible in one case.

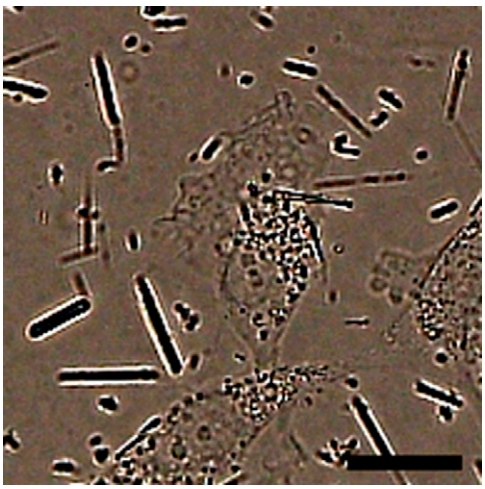

Movie S1. MeT5A mesothelial cells internalized Cro.

Movie S1

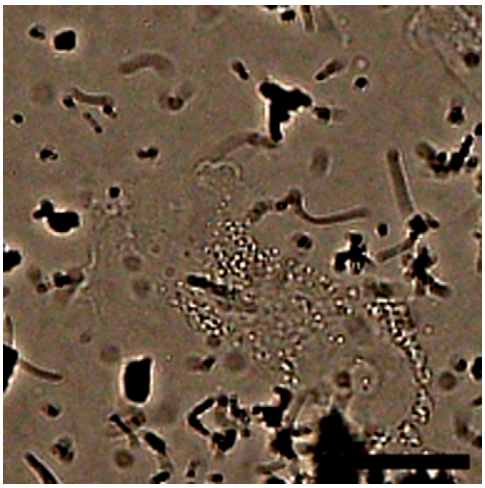

Movie S2. MeT5A mesothelial cells did not internalize NT115.

Movie S2

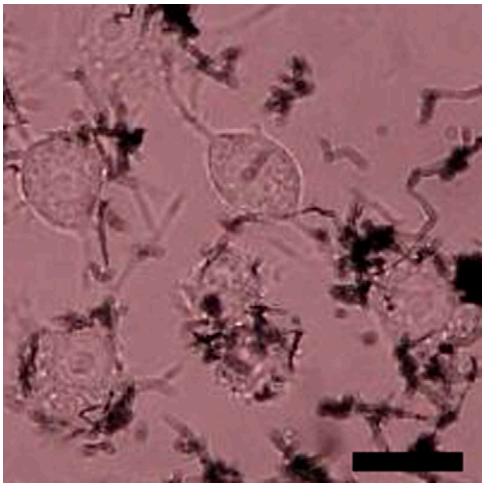

Movie S3. RAW264.7 macrophages phagocytosed NT145.

Movie S3

Movie S4. RAW264.7 macrophages did not phagocytose NTtngl.

Movie S4